Hindawi
International Journal of Chemical Engineering
Volume 2023, Article ID 7756174, 17 pages
https://doi.org/10.1155/2023/7756174

Research Article

An Experimental Analysis of Lean Binary Mixture Segregation in a Continuous Liquid Fluidized Bed

S. Narasimha Reddy [1] **and M. Venkata Ratnam** [2]

[1] *Department of Chemical Engineering, Rajalakshmi Engineering College, Chennai 602105, India*
[2] *Department of Chemical Engineering, Mettu University, Metu, Ethiopia*

Correspondence should be addressed to M. Venkata Ratnam; venkata.rat@meu.edu.et

Received 16 February 2023; Revised 17 May 2023; Accepted 25 October 2023; Published 9 November 2023

Academic Editor: Andreas Bück

This study examined the phenomenon of particle segregation in lean-phase binary mixtures, with a specific focus on the effect of particle size variations while flowing over a continuous liquid fluidized bed (LFB). The experimental configuration included a cylindrical column with a 72 mm internal diameter and 3 m vertical height. The binary mixture considered for this investigation was made up of solid materials that were rich in flotsam and jetsam. The study encompassed various factors, including liquid velocity, solid feed rate, and feed composition, in order to examine the separations containing flotsam and jetsam. A segregation index was calculated for each of the various combinations. On the other hand, the fluidization of the blend consisting of two solid components displayed notable differences in its behavior when compared to the reported effects of particle separation in any of the mixtures. Empirical correlations have been employed to establish relationships between variables, particularly with respect to solid entrainment and top and bottom product purity levels.

1. Introduction

The mineral processing industries employ various techniques for separation, including vibration-based separation (jigging), mechanical separation using screens (screening), gravity separation, and magnetic separation. Gravity separation is employed in various industrial processes as it is inherently simple, effective, and economical [1, 2]. A range of devices is available for the purpose of particle separation. The selection of equipment is influenced by various factors, including the physical properties of solid materials, the economics of the process, and the desired purity and recovery of valuable products. In contrast to alternative classifiers, fluidized bed classifiers exhibit a consistent and precise separation capability. The process of fluidization results in the segregation of solid particles of diverse size ranges and densities. Particles that ascend are commonly referred to as "flotsam," whereas particles that descend are commonly referred to as "jetsam." The literature employs batch or semibatch techniques for liquid fluidized beds (LFBs) [3–5]. There is presently a dearth of published literature concerning the elimination of fine and coarse particles in LFB systems. The hydrodynamic model proposed by Chen et al. [3] offers an elucidation for the voidage and particle dispersion phenomena observed in a continuous LFB classifier. This specific model is distinguished by the inclusion of a single parameter, which is fitted during the analysis process. This parameter is known as the axial dispersion coefficient. The current model lacks calculations for fractional recovery and purity of both products. The study conducted by Gavin et al. [4] investigated the practical application of teetered bed separators in the context of thick media separation. The authors have also furnished an elucidation on semibatch LFBs.

The LFB separator is capable of effectively separating microscopic particles from larger particles while maintaining the suspension of the bed. In the mineral industry, LFBs are employed for the purpose of sorting solid particles. The determination of the terminal settling velocity or transit velocity of an individual particle is crucial for the process of

solid materials segregation in LFBs [5–11]. Heavy minerals, also known as metals and metal oxides, are infrequently found in natural occurrences. It is common to engage in the process of extracting a small amount of high-value material from a large quantity of low-value material. This process necessitates a significant quantity of feed material to be continuously supplied to LFBs, where the inherent characteristics of solid components facilitate the separation of minerals. This approach has demonstrated efficacy in the beneficiation of gold, copper, and coal [6].

Limited research has been conducted on the topic of continuous gas fluidization employing lean-phase mixtures. The present study employed binary feed mixtures comprising significant levels of impurities to successfully separate mixtures of low-density minuscule particles within a continuous LFB system. The aim of this study was to examine the influence of operational conditions on the purity and yield of the products. The critical operational factors in this specific scenario encompass the rate of solid feed introduction and the velocity of the liquid surface. This study conducted an evaluation of the phenomena of entrainment, discharge rate, product purity, and pressure drop. Empirical correlations have been established to demonstrate the relationship between entrainment rate and product purity in binary mixtures containing impurities. This study introduces a novel methodology for the continuous separation of solid materials in LFBs and lean-phase mixtures.

2. Experimental Setup

The experimental setup is a continuous LFB employed in this study which followed the methodology outlined in previous investigations conducted by the author [5, 6]. The setup is a cylindrical perspex column with 72 mm internal diameter and 3 m height. The experimental setup comprised of two collecting tanks positioned at the top and bottom extremities of the primary column. The tanks were employed to facilitate the continuous extraction of solid materials, while preserving the undisturbed state of the bed conditions within the column. The feeding technique employed in this investigation involves the utilization of a cylindrical hopper to introduce a binary combination of materials into the column. The transfer of solid materials from the hopper to the primary column is facilitated through precalibrated scales. The flow rate of fluid media i.e., water was measured by rotameters. The feed input position is determined by the upper region. This study seeks to determine the best feed intake pipe placement near the top discharge parts. One pressure tap was carefully placed above the distributor plate and the other near the top discharge section. The differential manometer measured the column's collective pressure reduction using the taps. The higher and lower discharge parts were used to evaluate solid entrainment and discharge rate. Table 1 shows the physical properties of the solid materials used in this study. The particle size measurement was conducted using sieve analysis by employing Jayant standard test sieves on a singular sample. The current study examined two separate groups of particles with varying sizes, distinguished by size ratios of 2 and 3.35, respectively. This investigation was conducted within the framework of a continuous LFB. In this specific context, the feed exhibits a considerable flotsam, primarily comprising small particles. The feed also displays a significant amount of jetsam, characterized by a higher proportion of larger particles. The operating parameters utilized in the current study are presented in Table 2.

The column underwent controlled water inflow at a predetermined rate after determining the composition of a solid mixture. The solid materials that were already present in the hopper were transferred into the column using a preexisting scale. This scale had been calibrated to ensure a consistent flow rate of solid materials. The column was permitted to reach a state of equilibrium, as evidenced by the observed consistent decrease in pressure on the manometer. The validation of the steady state condition was accomplished by employing mass balancing principles. This required careful investigation of top and bottom solid materials flow rates and input rates. Once a state of equilibrium was achieved, the rates of solid flow were measured at both the upper and lower sections. In addition, samples were collected from each stream in order to assess their respective purities. Table 2 displays the range of operational parameters that were employed in the current study.

3. Results and Discussion

This study evaluated solid materials segregation in a continuous LFB employing lean mixes, binary feed combinations of solid materials with different sizes and densities, including flotsam-rich and jetsam-rich mixtures. Solids segregation depends on surface liquid velocity, solid feed rate, and feed composition. Entrainment, discharge, purity, and recovery of top and bottom products depend on these parameters [7, 8]. The ratio of fine particles in the overflow to total particles in the top flow determines the top product's purity. However, recovery is the weight of tiny particles in the overflow divided by the input flow weight [9]. The "top product" is small particles while the "bottom product" is bigger particles.

3.1. Flotsam-Rich Binary Mixtures

3.1.1. Influence of Liquid Velocity. Figures 1–14 depict the fluidization characteristics of flotsam-rich binary mixtures (size ratio of 2 and 3.35). These figures pertain to a specific feed entry location and assume identical densities for the solid materials in question. Figures 1 and 8 illustrate that the pressure drop initially reaches a peak before gradually diminishing and declining. The binary mixture with a high concentration of flotsam is characterized by a feed that primarily consists of fine particles, with a minor proportion of coarser particles. In low-liquid velocity conditions, fine particles exhibit an upward tendency, whereas a fraction of fine particles and a small quantity of coarser particles undergo sedimentation towards the bottom. The pressure drop experiences an increase at this particular location. As the velocity of the liquid increases, a limited quantity of fine particles becomes trapped, while other particles within the

Table 1: The physical characteristics of solid materials employed.

Material	d_p (mm)	ρ_s (kg/m^3)	U_{mf} (m/s)	U_t (m/s)
Glass beads	1.09	2490	0.0091	0.1674
Glass beads	2.18	2490	0.0238	0.274
Glass beads	3.67	2490	0.0386	0.372

Table 2: The operating variables and their ranges used.

Variable of the study	Range
U_L (m/s)	0.11–0.33
F (kg/h)	64–108, 58–93, and 141–175
x_f (%)	0.1 and 0.9
Z (m)	1.0

column undergo fluidization. By ensuring a slightly higher liquid velocity than the transport velocity of fine particles, the acting drag forces are enhanced, leading to the entrainment of a significant portion of the fine particles. As a result, the rate of pressure drop reduction is gradual. As the velocity of the liquid increases, it results in the entrainment of all fine particles and a continuous decrease in pressure drop. At increased liquid velocity, the larger particles are entrained with the smaller particles and expelled from the column. The bed seems to be functioning as a pneumatic transport system in its current condition. When the liquid velocity reaches a critical level and with enhanced solid feed rate, the pressure drop reaches its maximum value for the selected particle size ratios [10, 11].

Figures 2 and 9 show how liquid velocity affects the entrainment rate for a certain feed site, considering solid materials rate and particle size ratios. At any solid feed rate, entrainment reaches its maximum and then steadies as liquid velocity rises. A few tiny particles can be entrained at low liquid velocity, while others settle to the bottom with coarser particles. The entrainment rate is modest. Increased liquid velocity increases fine particle escape from the column, increasing the entrainment rate [6]. At the critical liquid velocity, entrainment is highest. Entrainment stabilizes above this velocity. Similar results were seen for 2 and 3.36 size ratios. At the critical liquid velocity, increasing the solid materials feed rate maximizes entrainment for both size ratios. Discharge rate and liquid velocity are shown in Figures 3 and 10 for various solid input rates and size ratios. The observed entrainment rate trends were the reverse.

Figures 4 and 11 show how liquid velocity affects the highest product purity at different solid feed rates. The experimental results showed that increasing liquid velocities decreased top product purity regardless of the solid feed rate. At low liquid velocity, small particles may be swept away, resulting in the purest top product. When liquid velocity exceeds fine particle transport velocity by a tiny margin, a considerable amount of fine particles become entrained and a small number of coarser particles are carried to the top section with the fine particles. The finished product loses purity. At higher liquid velocities, coarser particles are entrained with tiny particles. Thus, product quality suffers. The top product is purest at two size ratios, higher solid feed

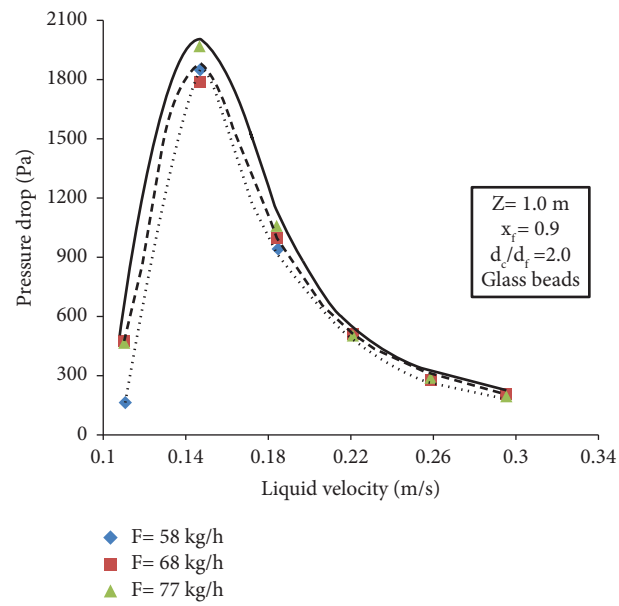

Figure 1: The influence of liquid velocity on the pressure drop at various solid feed rates for flotsam-rich binary mixtures with $d_c/d_f = 2$.

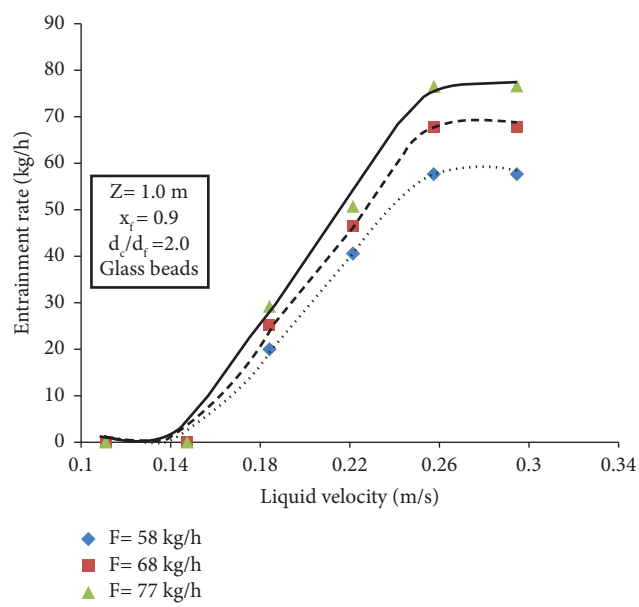

Figure 2: The influence of liquid velocity on entrainment rate at various solid feed rates for flotsam-rich binary mixtures with $d_c/d_f = 2$.

rates, and key liquid velocities. The top product is purest at a low solid materials feed rate, crucial liquid velocity, and size ratio of 3.36.

Figures 5 and 12 show how liquid velocity affects bottom product purity at different solid feed rates and size ratios. The experimental profiles show that increasing liquid velocity improves bottom product purity regardless of solid feed rate or particle size ratio. The settling of tiny particles with coarser particles reduces bottom product purity at low liquid velocity for any solid input rate. As liquid velocity rose, tiny particles

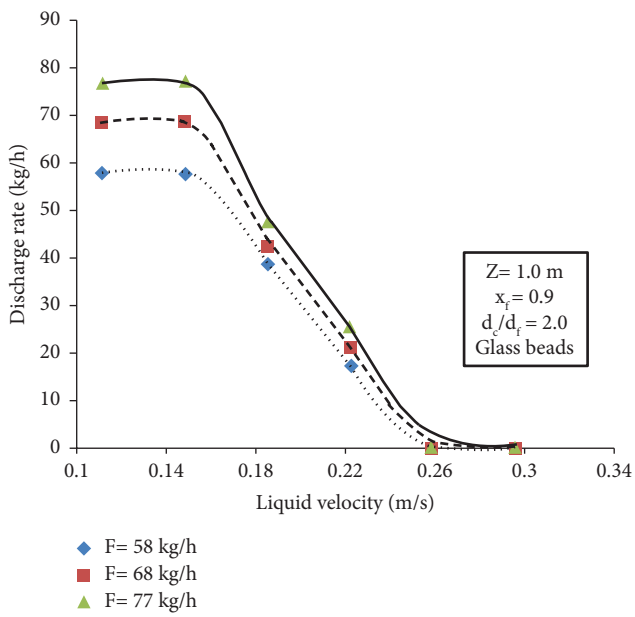

Figure 3: The influence of discharge rate on entrainment rate at various solid feed rates for flotsam-rich binary mixtures with $d_c/d_f = 2$.

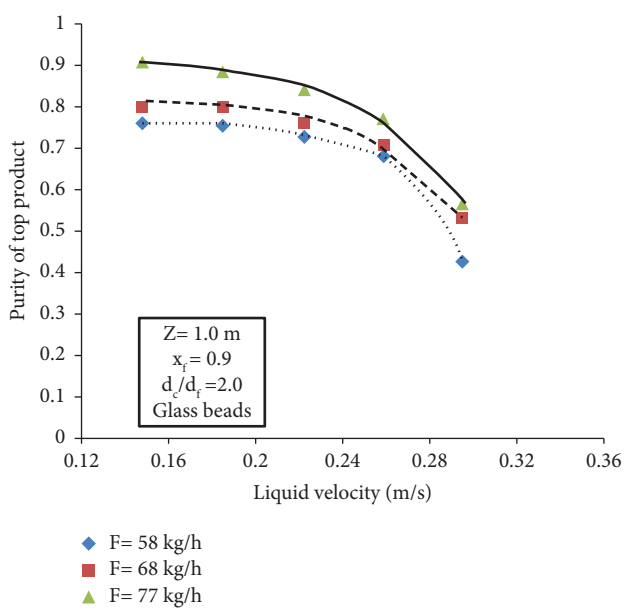

Figure 4: The influence of liquid velocity on the purity of top products at various solid feed rates for flotsam-rich binary mixtures with $d_c/d_f = 2$.

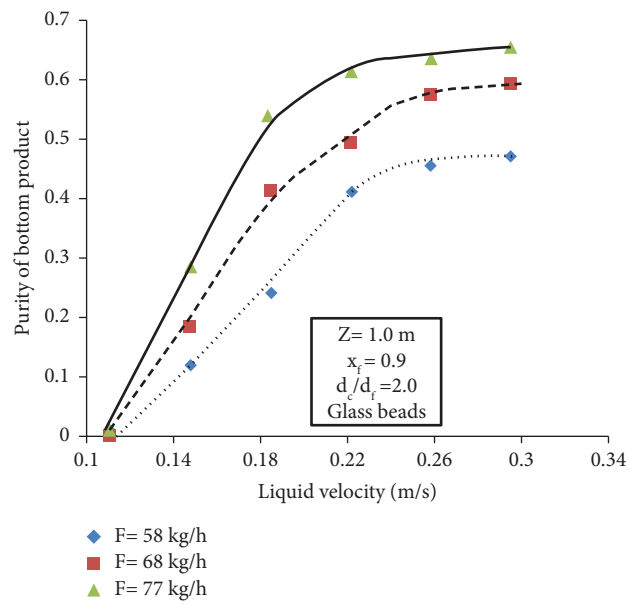

Figure 5: Effect of liquid velocity on purity of bottom product at different solid feed rates for flotsam-rich binary mixtures with $d_c/d_f = 2$.

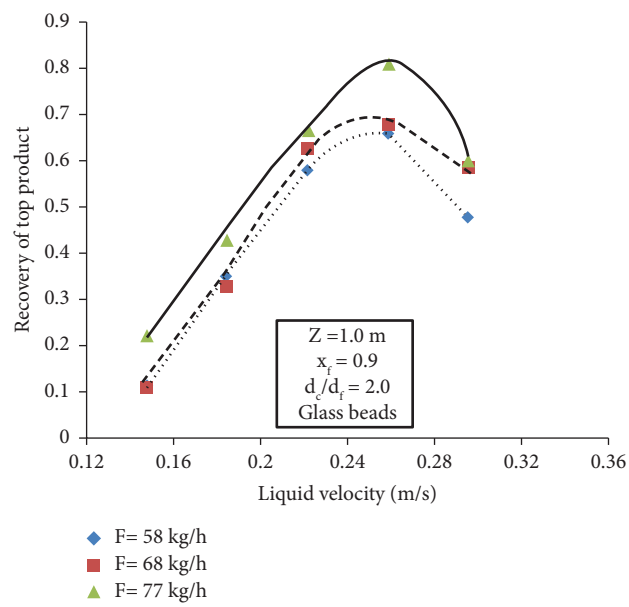

Figure 6: Effect of liquid velocity on recovery of top product at different solid feed rates for flotsam-rich binary mixtures with $d_c/d_f = 2$.

were entrained out of the column, leaving only coarser particles. Under these conditions, the lesser product improves. Increased liquid velocity can carry bigger particles out of the column. As a consequence, bottom product purity peaks and stabilizes. Both size ratios followed similar trends. At the critical liquid velocity, increasing the solid feed rate optimizes bottom product purity for both size ratios.

Figures 6 and 13 show top product recovery changes at a single feed site due to solid feed rates and particle size ratios. As liquid velocity rises for every solid input rate, top product recovery increases. However, it peaks before falling. Low liquid velocity limits particle entrainment, resulting in a low entrainment rate. Thus, this low entrainment rate suggests limited top product recovery. As liquid velocity rises, particle entrainment increases, increasing top product recovery. Entrainment and top product recovery peak at the crucial liquid velocity. At velocities over this threshold, entrainment and top product purity decrease, reducing recovery efficiency. Comparable size ratio trends were found. The particle size ratio determines the best top product recovery conditions. Higher solid feed rates and critical

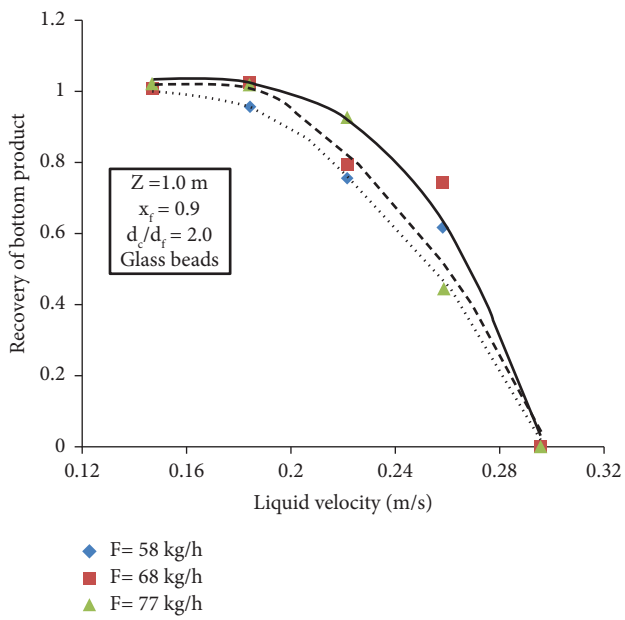

Figure 7: Effect of liquid velocity on recovery of bottom product at different solid feed rates for flotsam-rich binary mixtures with $d_c/d_f = 2$.

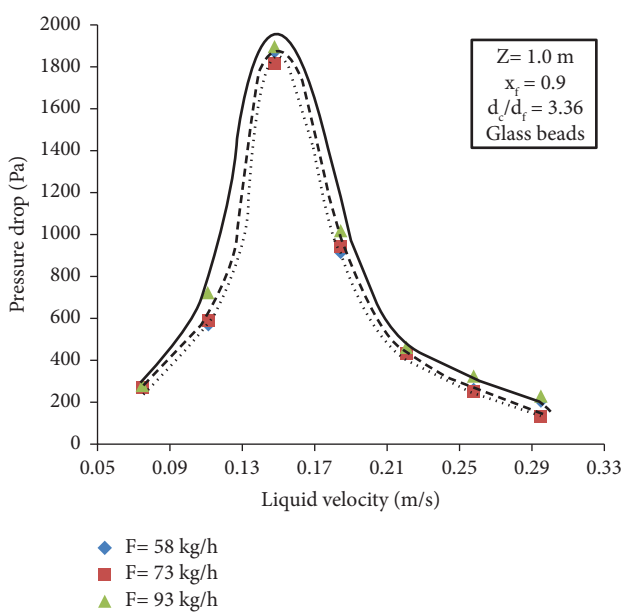

Figure 8: The influence of liquid velocity on pressure drop at several solid feed rates for flotsam-rich binary mixtures with $d_c/d_f = 3.36$.

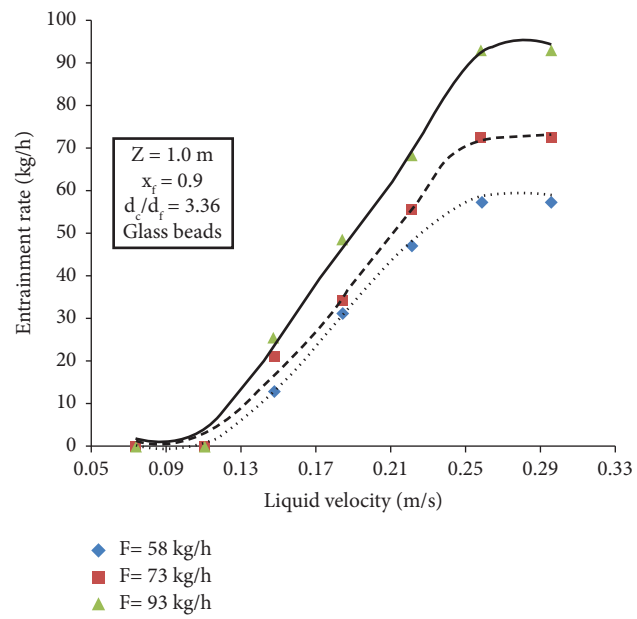

Figure 9: The influence of liquid velocity on entrainment rate at several solid feed rates for flotsam-rich binary mixtures with $d_c/d_f = 3.36$.

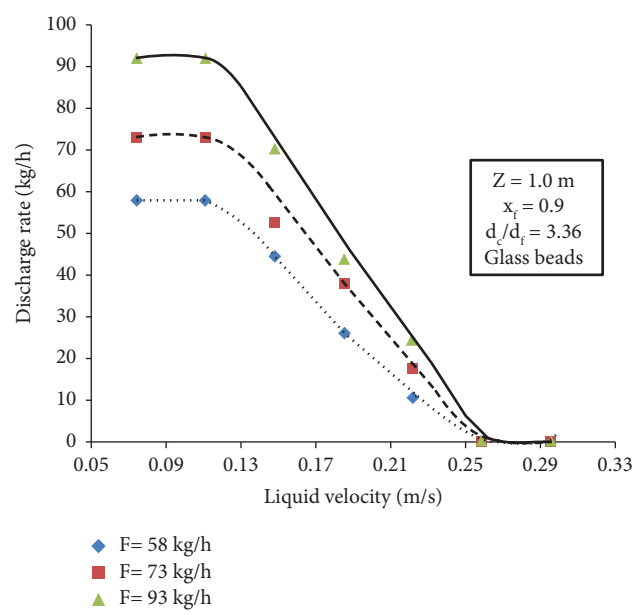

Figure 10: The influence of liquid velocity on discharge rate at various solid feed rates for flotsam-rich binary mixtures with $d_c/d_f = 3.36$.

liquid velocities maximize top product recovery for a particle size ratio of 2. At lower solid feed rates and the same critical liquid velocity, top product recovery is best at a particle size ratio of 3.36.

Figures 7 and 14 show how liquid velocity affects bottom product retrieval at different solid feed rates and size ratios. As liquid velocity and solid feed rate rise, bottom product recovery decreases to lower liquid velocities, many particles sink to the bottom. Thus, the discharge rate increases, maximising bottom product recovery. Larger particles are entrained with smaller particles at higher liquid velocities, reducing the discharge rate. Retrieving the lesser product has little utility. Both size ratios showed similar trends. Increased solid feed rates boost bottom product recovery at crucial liquid velocity. Both size ratios follow this pattern.

3.1.2. Influence of Solid Feed Rate. Figures 15–22 depict the influence of solid feed rate on the fluidization process of a binary mixture containing a significant quantity of flotsam. Figures 15 and 19 illustrate that increasing the solid materials

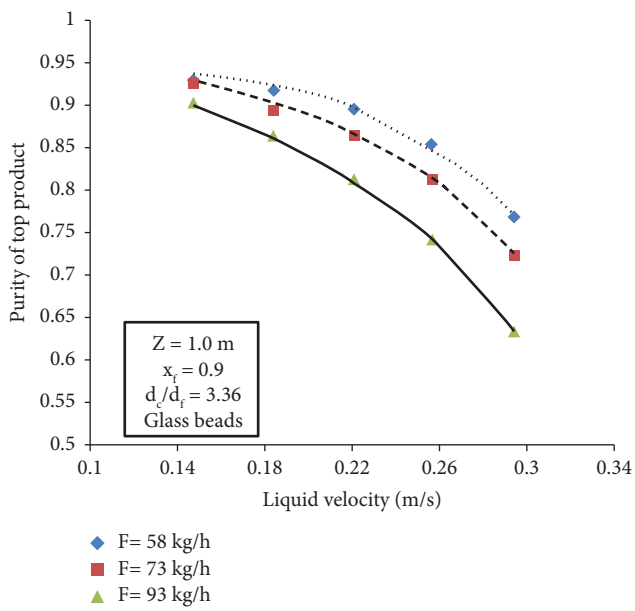

Figure 11: Effect of liquid velocity on purity of top product at different solid feed rates for flotsam-rich binary mixtures with $d_c/d_f = 3.36$.

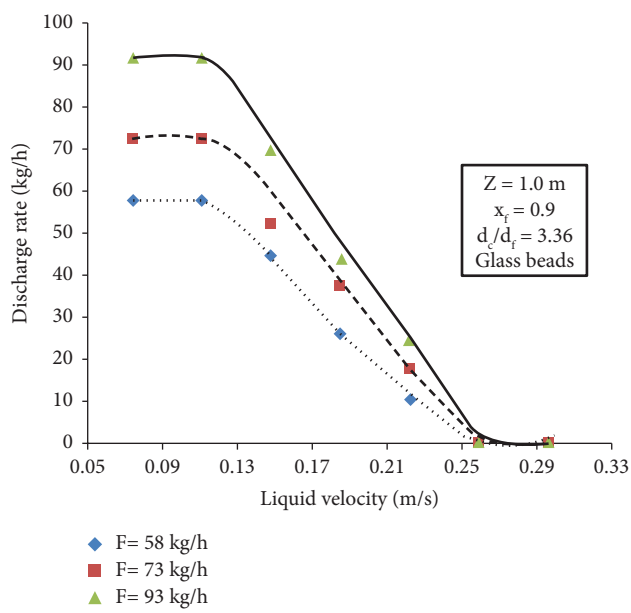

Figure 12: Effect of liquid velocity on purity of bottom product at different solid feed rates for flotsam-rich binary mixtures with $d_c/d_f = 3.36$.

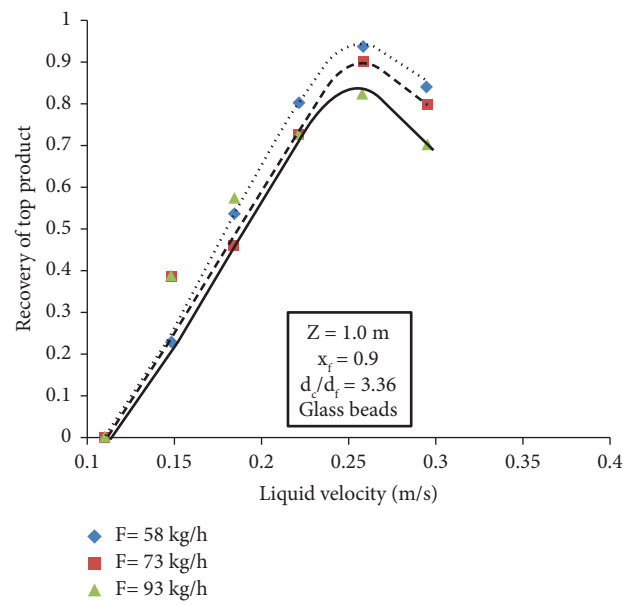

Figure 13: The influence of liquid velocity on recovery of top product at various solid feed rates for flotsam-rich binary mixtures with $d_c/d_f = 3.36$.

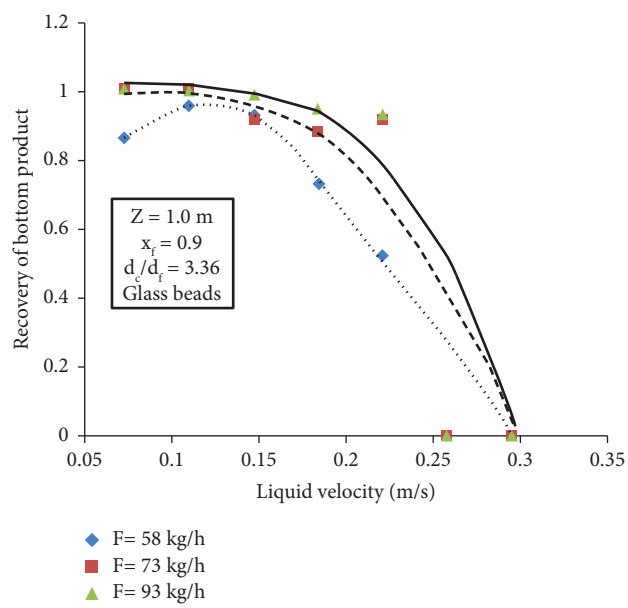

Figure 14: Effect of liquid velocity on recovery of bottom product at different solid feed rates for flotsam-rich binary mixtures with $d_c/d_f = 3.36$.

feed rate results in higher top product purity at a given liquid velocity, when the particle size ratio is 2. An increase in the solid materials feed rate leads to a decrease in the purity of the top product when the particle size ratio is 3.36. Optimal conditions for attaining maximum product purity are typically associated with low liquid velocity and solid input rate. This is because certain tiny particles entrain immediately. When liquid velocity is low, increasing solid feed rate increases column particle holdup. This context prioritizes fine particle concentration above coarse particle concentration. The top product is purest with greater solid feed rates and low liquid velocities for a particle size ratio of 2. At low liquid velocities and solid feed rates, the top product is purest at a 3.35 particle size ratio.

Figures 16 and 20 show that bottom product purity changes with solid feed rates, liquid velocities, and size ratios. These observations concern a feed input point. According to the results, the bottom product purity rises with solid feed rate, regardless of liquid velocity and size ratios. The bottom product is less pure at low liquid velocities and solid feed rates. Low liquid velocities cause a lot of small particles to settle to the bottom. The column has more particles when the solid feed rate is raised and the bed

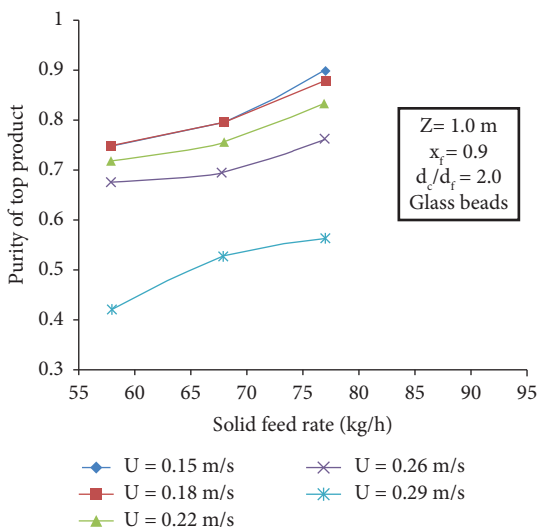

Figure 15: The influence of solid feed rate on the purity of top product at various liquid velocities for a binary mixture containing a significant quantity of flotsam with $d_c/d_f = 2$.

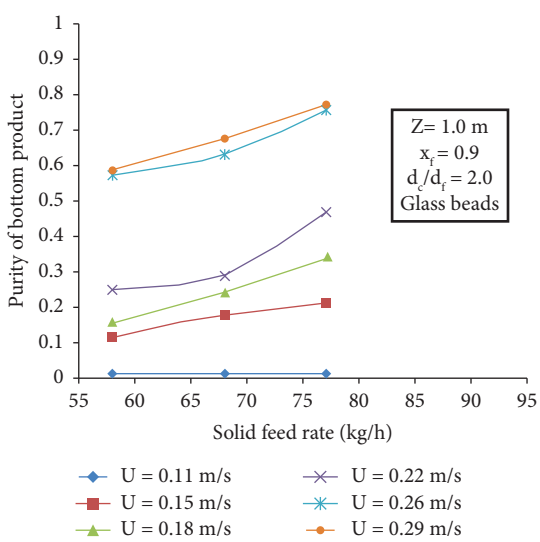

Figure 16: The influence of solid feed rate on the purity of the bottom product at various liquid velocities containing a significant quantity of flotsam with $d_c/d_f = 2$.

is operated at low liquid velocity. This causes particle-particle interactions, which make particles autonomous and resist settling. Since there is no vertical movement in the column, the bottom product progressively becomes purer. Increased liquid velocity and solid input rate entrain a large fraction of particles, resulting in the purest bottom product. This is true for both size ratios as increased solid feed rate and liquid velocity maximize bottom product purity.

Figures 17 and 21 show how solid feed rate affects top product recovery. These statistics show liquid velocities and size ratios for a single feed point. For both size ratios, unusual behavior was seen. At a particle size ratio of 2 and low liquid velocities, increasing the solid feed rate increases top product recovery. The entrainment rate decreases with solid feed rate, reducing top product recovery. Under high solid

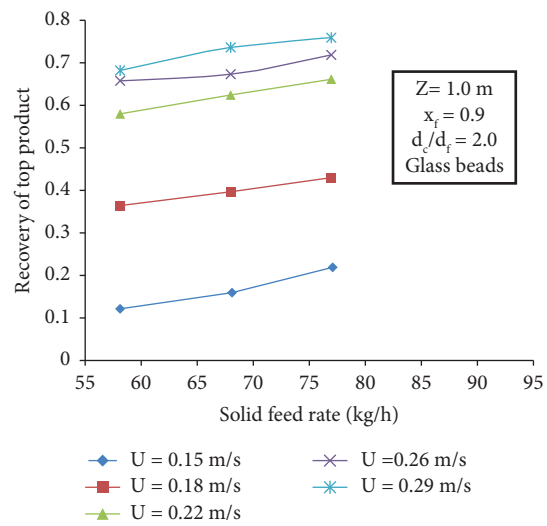

Figure 17: The influence of solid feed rate on recovery of top product at various liquid velocities containing a significant quantity of flotsam with $d_c/d_f = 2$.

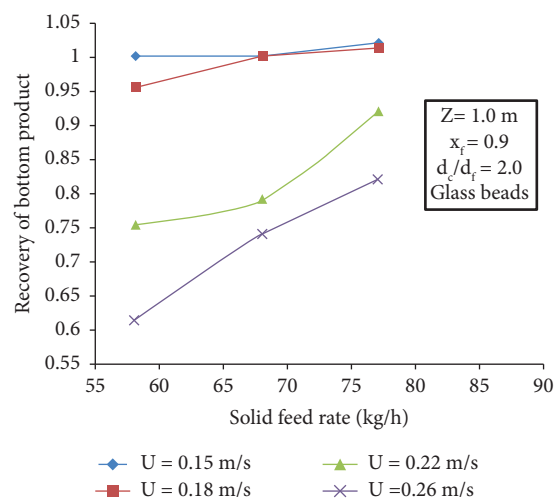

Figure 18: The influence of solid feed rate on recovery of bottom product at various liquid velocities containing a significant quantity of flotsam with $d_c/d_f = 2$.

feed rate and liquid velocity, many particles become entrained and displaced from the column. Therefore, the leading product has the largest recovery value. The particle size ratio of 3.36 shows an inverse trend.

Figures 18 and 22 show how solid feed rate affects bottom product recovery. These figures focus on a single feed entrance site and liquid velocities and size ratios. According to the figures, increasing the solid feed rate at any liquid velocity increases bottom product recovery for both particle size ratios. Low liquid velocity and solid input rate cause most column particles to be fine. A small fraction of tiny particles become entrained at this velocity, while the rest settle to the bottom. The discharge rate rises. Due to the impact, bottom-up product recovery has risen. When liquid velocities are low and solid input rates are high, column solid materials accumulate. In this setting, solid materials recirculation in the column and particle interactions is more

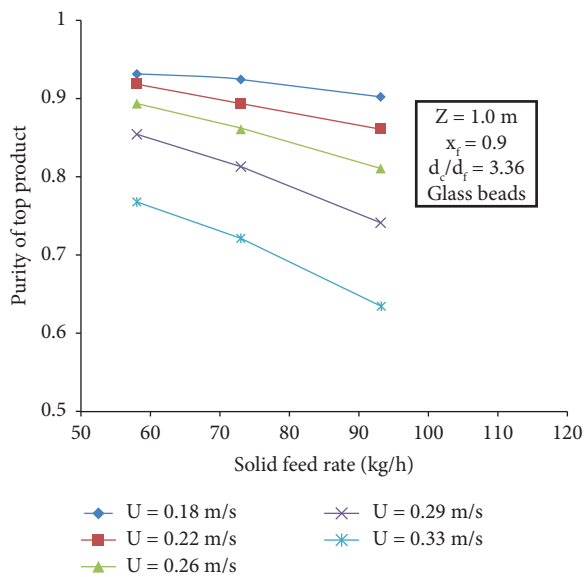

Figure 19: The influence of solid feed rate on the purity of top product at various liquid velocities containing a significant quantity of flotsam with $d_c/d_f = 3.36$.

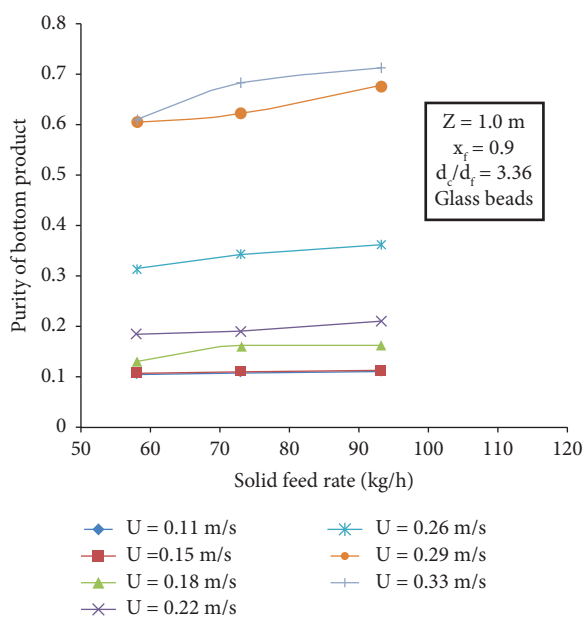

Figure 20: The influence of solid feed rate on the purity of the bottom product at various liquid velocities containing a significant quantity of flotsam with $d_c/d_f = 3.36$.

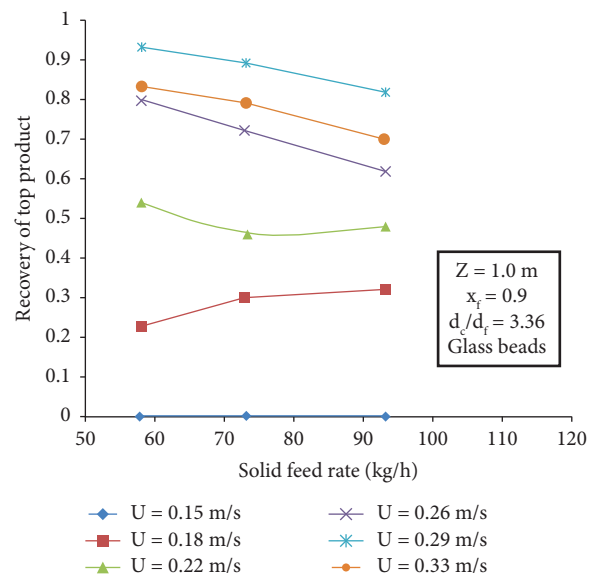

Figure 21: The influence of solid feed rate on recovery of top product at various liquid velocities containing a significant quantity of flotsam with $d_c/d_f = 3.36$.

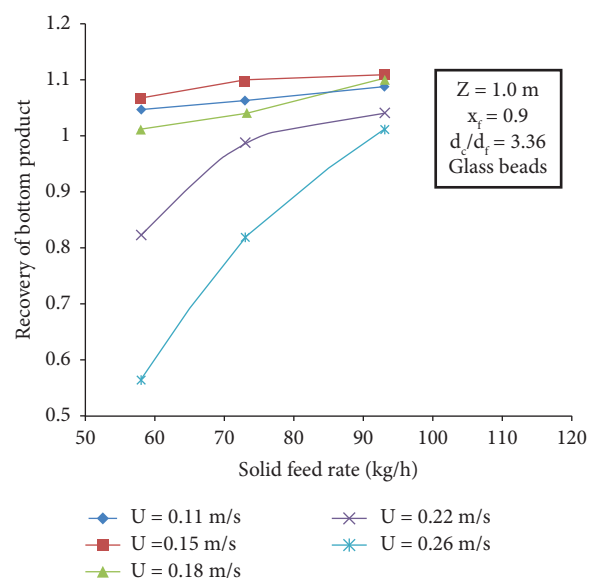

Figure 22: The influence of solid feed rate on recovery of bottom product at various liquid velocities containing a significant quantity of flotsam with $d_c/d_f = 3.36$.

important. Thus, particles move even at low liquid velocity to ascend and circulate in the column without settling. As a result of this, even with low liquid velocities, a larger solid feed rate optimizes bottom product recovery. This is true for both size ratios.

3.2. Jetsam-Rich Binary Feed Mixtures

3.2.1. Influence of Liquid Velocity. Figures 23–36 show jetsam-rich binary feed mixture fluidization. These data illustrate solid feed rates and size ratios for a certain feed site. Figures 23 and 30 show how liquid velocity affects pressure drop at different solid feed rates and particle size ratios. Figure 23 suggests that this study's phenomena are similar to those in binary feed combinations with a lot of flotsam. With a particle size ratio of 3.36, a rise in liquid velocity causes the pressure to decrease to peak, then decline, and then peak again before stabilizing. As liquid velocity rises, pressure drop increases. Therefore, maintaining liquid velocity above fine particle transport velocity is recommended as a large amount of fine particles will be entrained and transported away. Thus, the pressure drop will decrease, reducing coarser particle transport to the column's outer portion. As liquid

velocity rose, bigger particles tried to detach from the column. However, the lack of liquid drag caused these particles to fall, causing large column internal recirculations. A progressive rise in pressure decreases results. The entrainment of coarser particles increases when the velocity matches the transit velocity of bigger particles. As a result, pressure drops significantly. Similar to pneumatic transport, coarser and finer particles are entrained from the column and bed at higher liquid velocity.

Figures 24, 25, 31, and 32 demonstrate how the entrainment rate affects the discharge rate at a feed entry site with varying solid feed rates and particle size ratios. Figure 1 illustrates that entrainment peaks and stabilizes at 2 particle size ratio as liquid velocity rises. However, the discharge rate peaks at low liquid velocity and subsequently drops. Entrainment and discharge rates rise and decrease with a particle size ratio of 3.36. Entrainment and discharge rates peak at critical liquid velocity and rising solid feed rate with a particle size ratio of 2. Higher solid feed rates increase entrainment and discharge regardless of liquid velocity while maintaining a 3.36 particle size ratio.

Figures 26 and 33 show how solid feed rates and particle size ratios affect upper product purity. The data show that liquid velocity increases, reducing top product purity. Similar trends are seen in binary feed combinations with high flotsam concentrations. No matter the size ratio or liquid velocity, a low solid feed rate maximizes top product purity. Figures 27 and 34 show bottom product purity changes for a single feed entrance position over solid feed rates and particle size ratios. Regardless of particle size ratio and solid feed rate, liquid velocity increases bottom product purity. The purity of bottom product reaches maximum at a specified liquid velocity for both size ratios. The behavior is similar to binary mixes rich in flotsam. Increased solid feed rate maximizes bottom product purity regardless of liquid velocity.

Figures 28, 35, and 36 show how liquid velocity affects top and bottom product retrieval at different solid feed rates and size ratios. According to the figures, liquid velocity affects top product recovery. Specifically, when liquid velocity increases, top product recovery first rises but then falls. As liquid velocity rises, bottom product recovery decreases. Entrainment, discharge rate, and product purity affect top and bottom product recovery. Lower liquid velocities have less solid materials entrainment and greater solid materials discharge. Top-tier items have a low retrieval rate, whereas bottom-tier ones have a high rate. The entrainment rate increases top product recovery because liquid velocity increases the entrainment rate. Conversely, the discharge rate decreases, reducing bottom product recovery. Due to low purity, top product recovery decreases after a certain liquid velocity. At high liquid velocity, top and bottom product recovery is ineffective. The top product recovers more when the solid feed rate is low for a particle size ratio of 2. Regardless of liquid velocity, increasing solid feed rate increases bottom product recovery. The particle size ratio of 3.36 shows that increasing the solid feed rate increases top and bottom products' recovery independent of liquid velocity. Top and bottom product recovery followed similar size ratio tendencies.

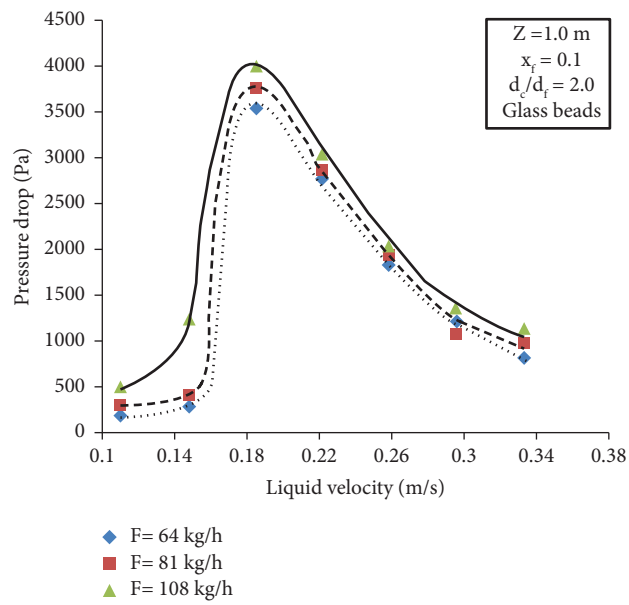

Figure 23: The influence of liquid velocity on pressure drop at various solid feed rates for a jetsam-rich binary feed mixture with $d_c/d_f = 2$.

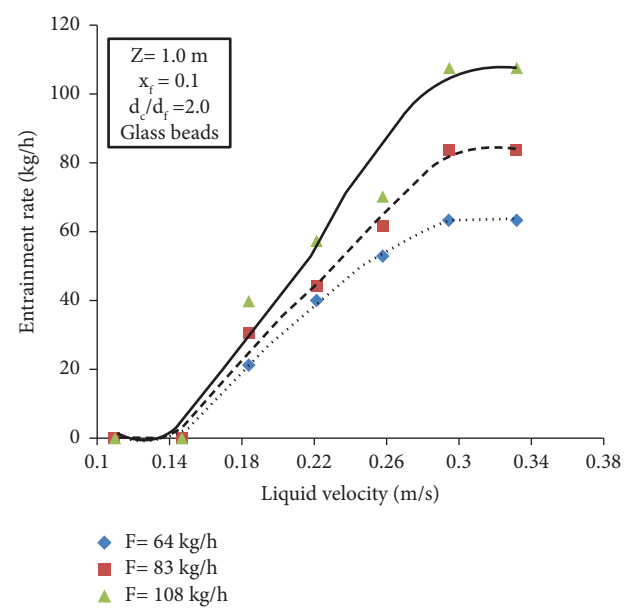

Figure 24: The influence of liquid velocity on entrainment rate at several solid feed rates for a jetsam-rich binary feed mixture with $d_c/d_f = 2$.

3.2.2. Influence of Solid Feed Rate. In Figures 37–44, solid feed rate impacts purity and recovery in a binary feed mixture with jetsam at varying liquid velocities and particle size ratios. These values show one feed entry. Figures 37 and 41 indicate that greater liquid velocities, regardless of solid

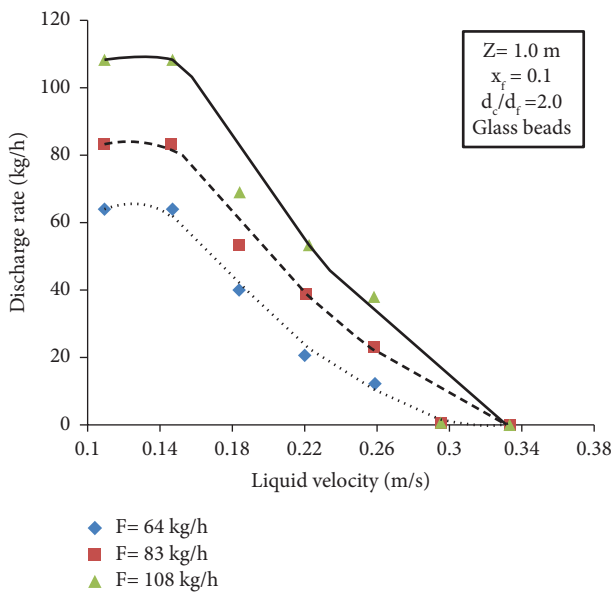

Figure 25: The influence of liquid velocity on discharge rate at several solid feed rates for jetsam-rich binary feed mixture with $d_c/d_f = 2$.

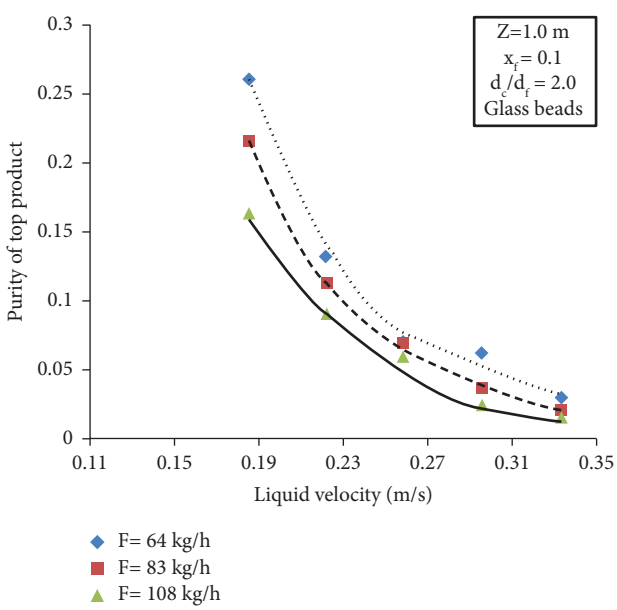

Figure 26: The influence of liquid velocity on purity of top product at several solid feed rates for jetsam-rich binary feed mixture with $d_c/d_f = 2$.

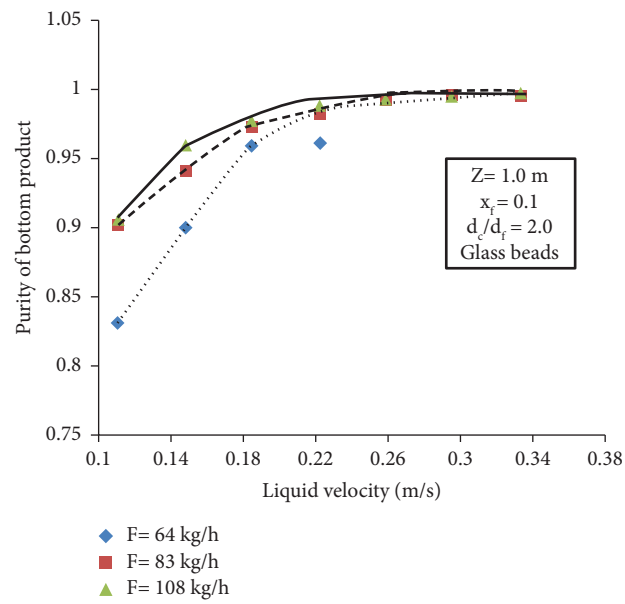

Figure 27: The influence of liquid velocity on the purity of the bottom product at several solid feed rates for a jetsam-rich binary feed mixture with $d_c/d_f = 2$.

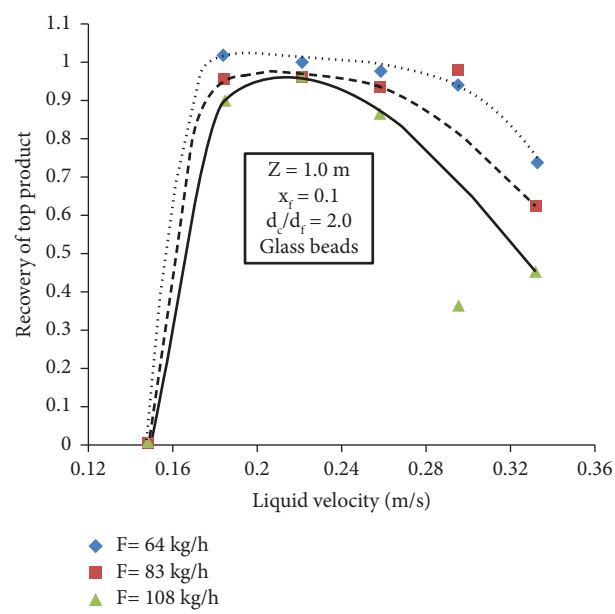

Figure 28: The influence of liquid velocity on recovery of top product at several solid feed rates for jetsam-rich binary feed mixture with $d_c/d_f = 2$.

input rate, reduce top product purity for both size ratios. Low liquid velocity and solid materials feed rate deliver little fines and courses into the column. Due to the top product's purity, even small particles may be entrained at low liquid velocity. Increased liquid velocity and solid input rate fill the column with larger particles. At this velocity, most larger particles cluster at the column top and high-end things suffer. The purest product is at low liquid and solid feed rates. It applies to both size ratios.

Figures 38 and 42 show how solid feed rate affects bottom product purity at different particle size ratios and liquid velocities. Low liquid velocity and solid feed rate reduce bottom product purity. This happens because most particles settle at the bottom. When solid feed is fed at a high rate and the bed is operated with a low liquid flow velocity, the bottom product's purity improves. When liquid velocity and solid feed rate are increased, many bigger particles entering the column are transported with the flow. Thus, the

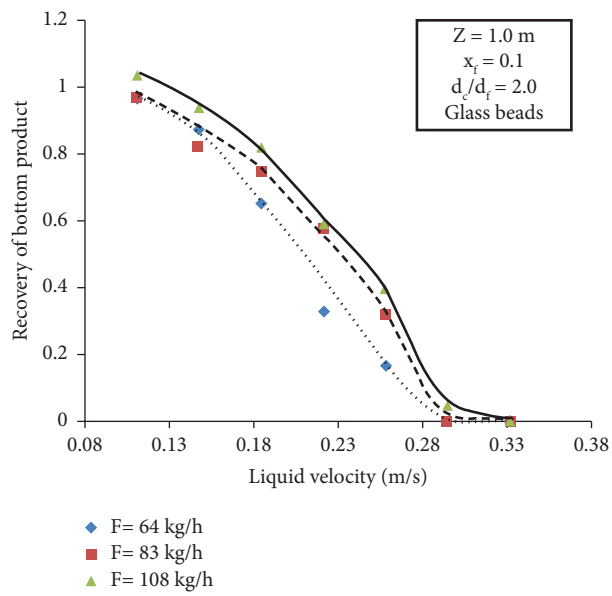

Figure 29: Effect of liquid velocity on recovery of bottom product at different solid feed rates for jetsam-rich binary feed mixture with $d_c/d_f = 2$.

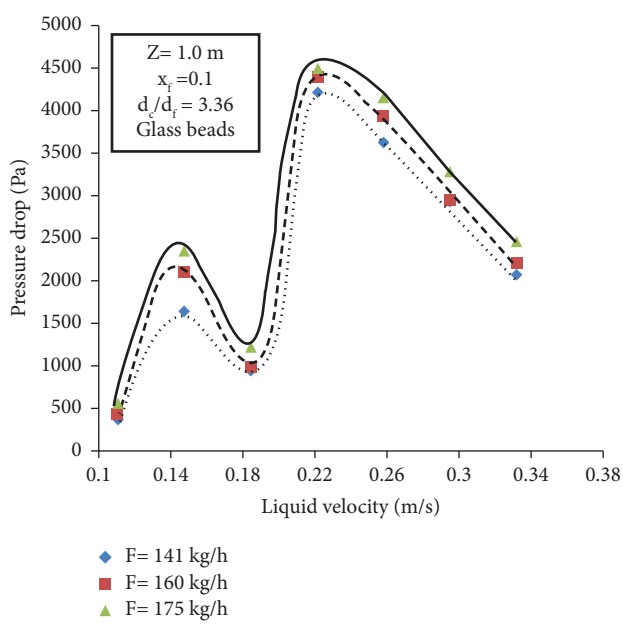

Figure 30: The influence of liquid velocity on pressure drop at several solid feed rates for a jetsam-rich binary feed mixture with $d_c/d_f = 3.36$.

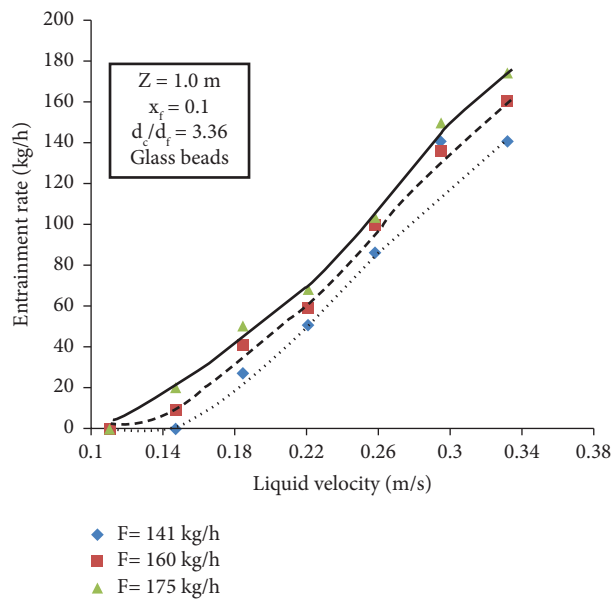

Figure 31: The influence of liquid velocity on pressure drop at several solid feed rates for a jetsam-rich binary feed mixture with $d_c/d_f = 3.36$.

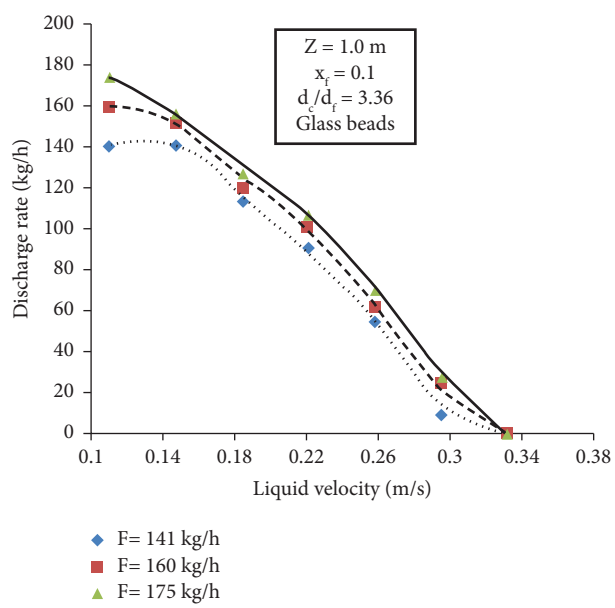

Figure 32: The influence of liquid velocity on discharge rate at several solid feed rates for a jetsam-rich binary feed mixture with $d_c/d_f = 3.36$.

bottom product's purity is ideal for both size ratios. At a size ratio of 2, a greater liquid velocity and medium solid feed rate provide the purest bottom product. Conversely, increased liquid velocity and solid input rate provide a pure bottom product.

3.3. Influence of Particle Size Ratio. Figures 45–48 show how feed composition affects flotsam and jetsam purity and recovery in binary feed combinations. Figures 45 and 46 show how feed composition affects top product purity at different liquid velocities. The feed content, especially tiny particles, improves product purity. This applies to both size ratios. Suboptimal feed composition and liquid velocity reduce top product purity and increase the feed mix to purify the top product. Even at low liquid velocities, adding tiny particles to the column increases entrained particle concentration or magnitude. When liquid velocities are high and feed compositions are low, fines entrained bigger particles damage to top product purity. However, higher

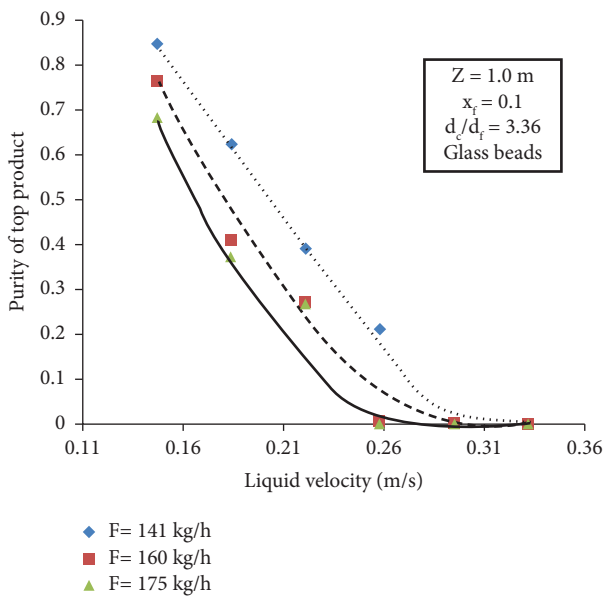

Figure 33: The influence of liquid velocity on the purity of top product at several solid feed rates for a jetsam-rich binary feed mixture with $d_c/d_f = 3.36$.

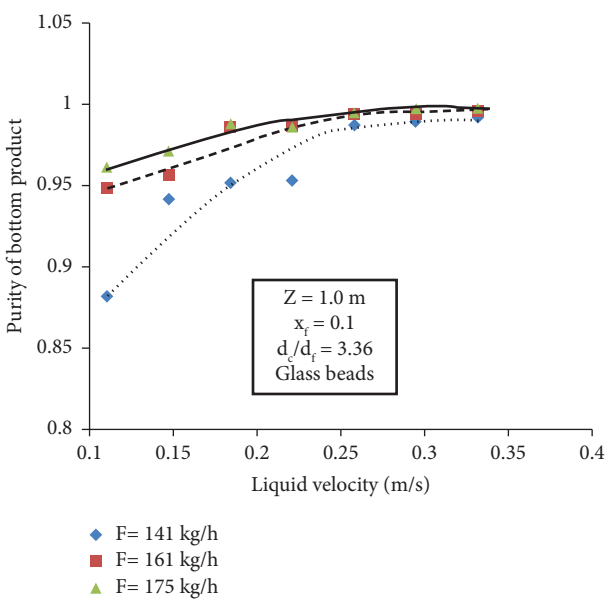

Figure 34: The influence of liquid velocity on the purity of the bottom product at several solid feed rates for a jetsam-rich binary feed mixture with $d_c/d_f = 3.36$.

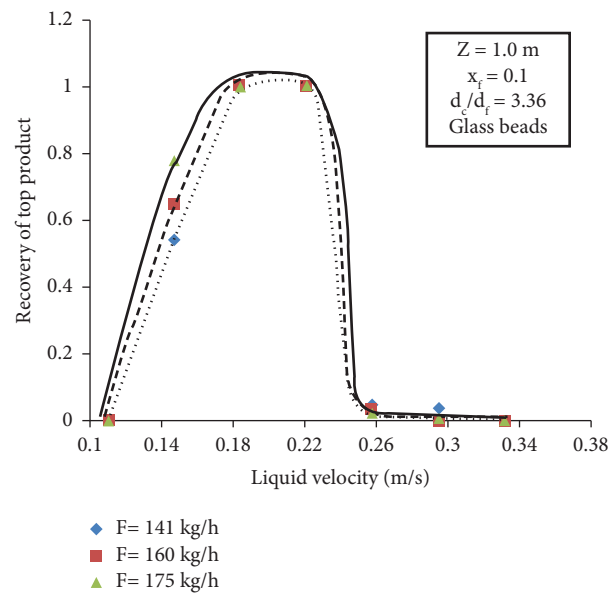

Figure 35: The influence of liquid velocity on recovery of top product at several solid feed rates for jetsam-rich binary feed mixture with $d_c/d_f = 3.36$.

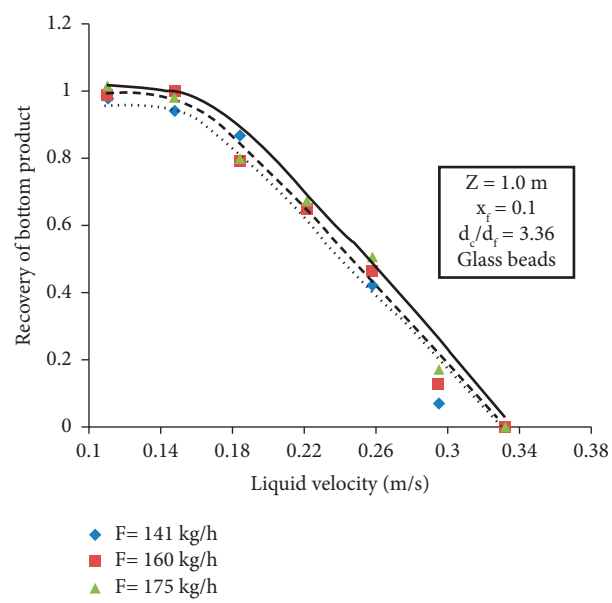

Figure 36: The influence of liquid velocity on recovery of bottom product at several solid feed rates for jetsam-rich binary feed mixture with $d_c/d_f = 3.36$.

feed compositions get more fine particles into the column than coarser particles. High liquid velocities provide the top product with the most purity and increase the feed composition and reduce liquid velocity while maintaining the solid feed rate and size ratio for maximum product quality.

Figure 46 shows how feed mix affects bottom product purity. The plots show liquid velocities and particle size ratios at the feed entrance. Figure 49 shows that liquid velocity does not affect bottom product purity. Under low liquid velocities and feed compositions, the bottom product is pure due to the absence of tiny particles and the presence of coarser particles entering the column. At the required velocity, some tiny particles are entrained and others are fluidized in the column. Therefore, product purity must be prioritized. Increased liquid velocity and feed mixture enhance column fine particle concentration. At greater liquid velocities, most tiny particles are eliminated, causing bigger particles to accumulate. The vertical flow of tiny particles expelled bigger particles in the column, purifying the bottom product. According to the study, lowering feed composition and boosting liquid velocity improve bottom product purity.

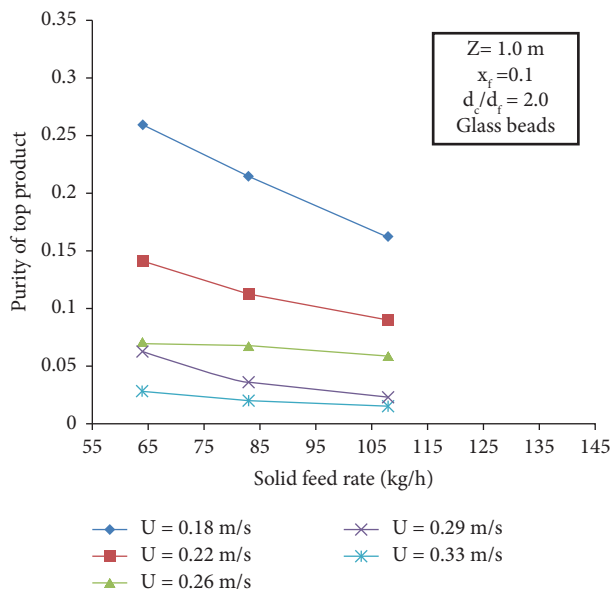

Figure 37: The influence of solid feed rate on purity of top product at several liquid velocities for a binary feed mixture with jetsam with $d_c/d_f = 2$.

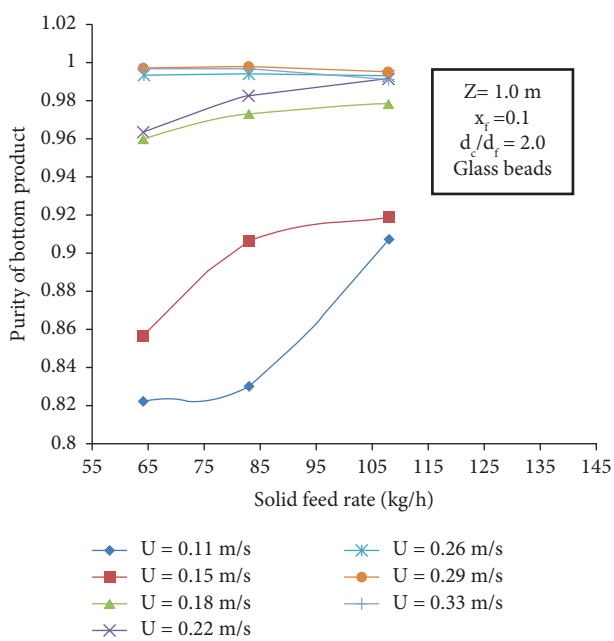

Figure 38: The influence of solid feed rate on the purity of the bottom product at several liquid velocities for a binary feed mixture with jetsam with $d_c/d_f = 2$.

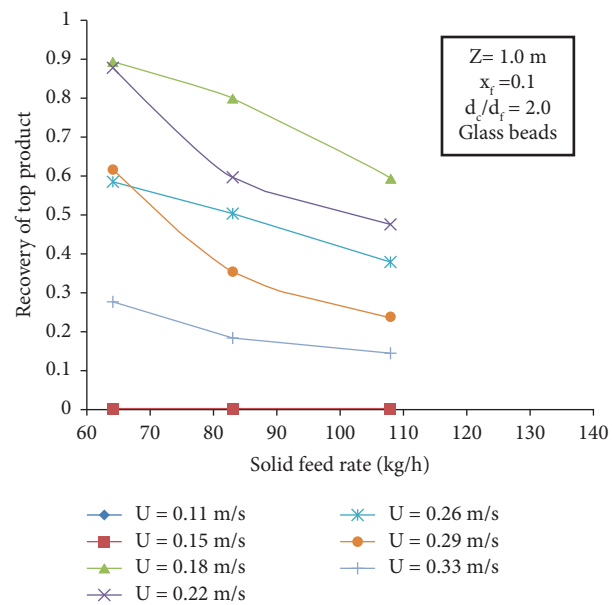

Figure 39: The influence of solid feed rate on recovery of top product at several liquid velocities for a binary feed mixture with jetsam with $d_c/d_f = 2$.

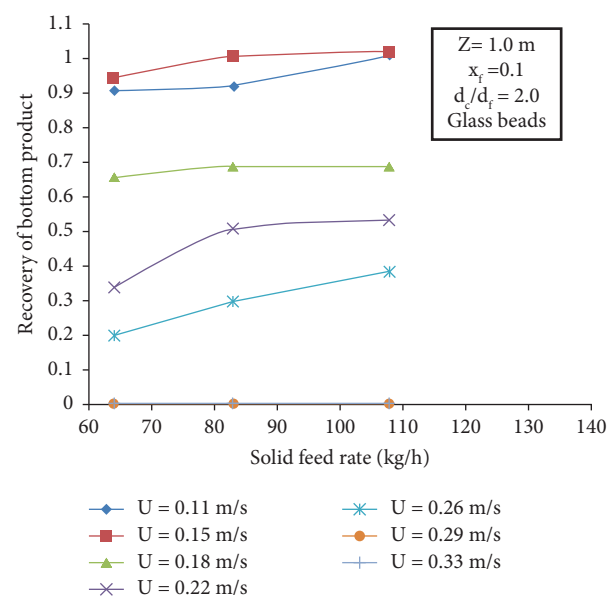

Figure 40: The influence of solid feed rate on recovery of bottom product at several liquid velocities for a binary feed mixture with jetsam with $d_c/d_f = 2$.

Figures 47 and 48 show that feed composition decrease reduces top product recovery independent of liquid velocity. Under low liquid velocity and feed composition, tiny particles become entrained and entrain faster. Under these settings, product retrieval optimization improves. Interestingly, the size ratio of 2 increases top product recovery under low liquid velocity and feed composition. When the size ratio is 3.34, liquid velocities rise and feed compositions drop, improving top product purity. Figure 48 shows how feed mix affects bottom product recovery at different liquid velocities and particle size ratios. The figure data showed a substantial link between feed mix and bottom product recovery, regardless of size ratio. Lower liquid velocities and bigger feed compositions boost bottom product recovery regardless of size ratios.

3.4. Empirical Correlations. The study reveals a positive correlation between the phenomenon of solid materials entrainment and both liquid velocity and solid materials feed rate in the systems characterized by a high presence of flotsam and jetsam. The correlation for the entrainment rate of solid materials, as determined from the experimental data

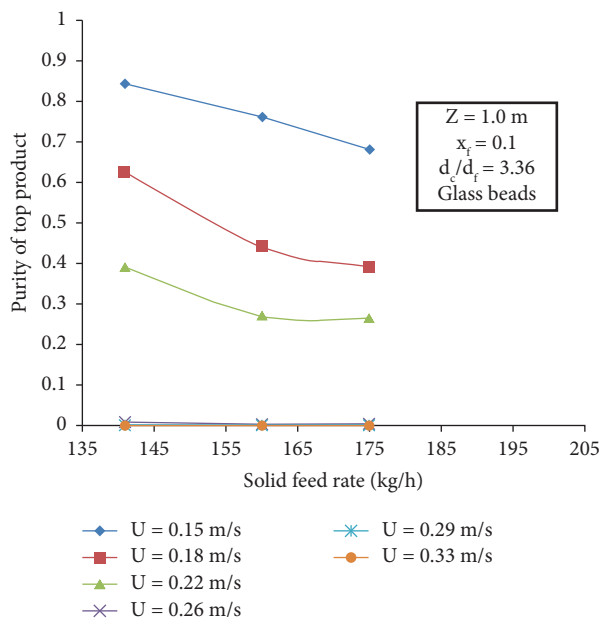

Figure 41: The influence of solid feed rate on purity of top product at several liquid velocities for a binary feed mixture with jetsam with $d_c/d_f = 3.36$.

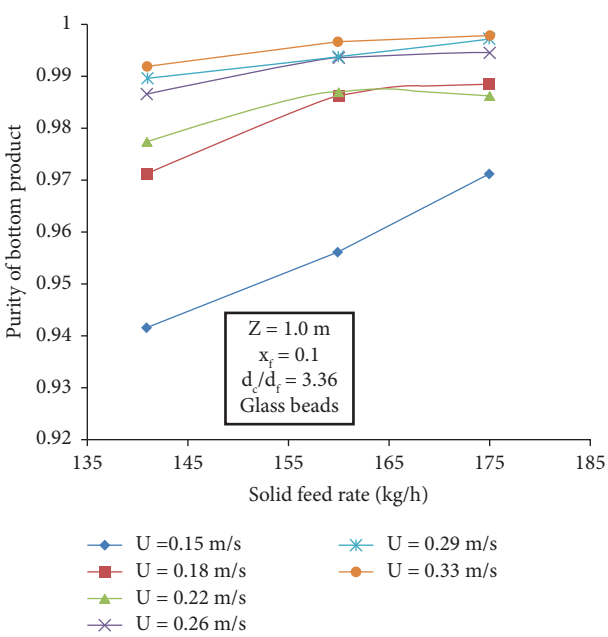

Figure 42: The influence of solid feed rate on the purity of the bottom product at several liquid velocities for a binary feed mixture with jetsam with $d_c/d_f = 3.36$.

obtained in this study, is established for size ratios of 1.68 and 2, as outlined in the following equation:

$$\frac{E}{F} = 0.511\left[\left(\frac{U_{t,c} - U_L}{U_{t,c} - U_{t,f}}\right)^{-0.478}(x_f)^{0.21}\left(\frac{Z}{Z_0}\right)^{-0.038}\right. . \quad (1)$$

As demonstrated in equation (2), the discharge rate of solid materials may be computed by subtracting the feed rate from the entrainment rate as follows:

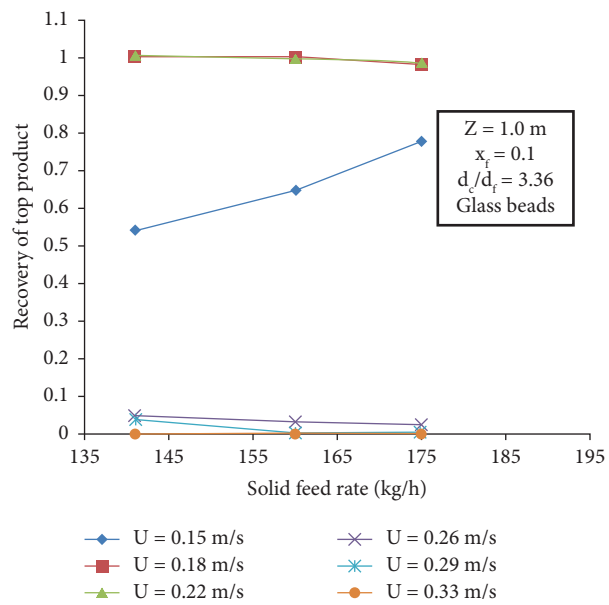

Figure 43: The influence of solid feed rate on recovery of top product at several liquid velocities for a binary feed mixture with jetsam with $d_c/d_f = 3.36$.

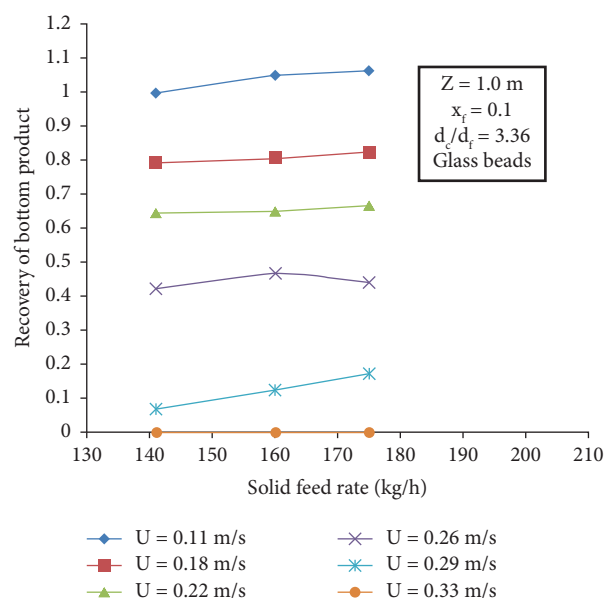

Figure 44: The influence of solid feed rate on recovery of bottom product at several liquid velocities for a binary feed mixture with jetsam with $d_c/d_f = 3.36$.

$$D = F - E. \quad (2)$$

The current study shows that the purity of the top product is negatively connected with liquid velocity and solid feed rate and positively correlated with feed particle composition across all combinations as shown in the following equation:

$$Y_f = 0.674\left[\left(\frac{U_{t,c} - U_L}{U_{t,c} - U_{t,f}}\right)^{0.53}(x_f)^{0.39}\left(\frac{Z}{Z_0}\right)^{-0.39}\right. \quad (3)$$

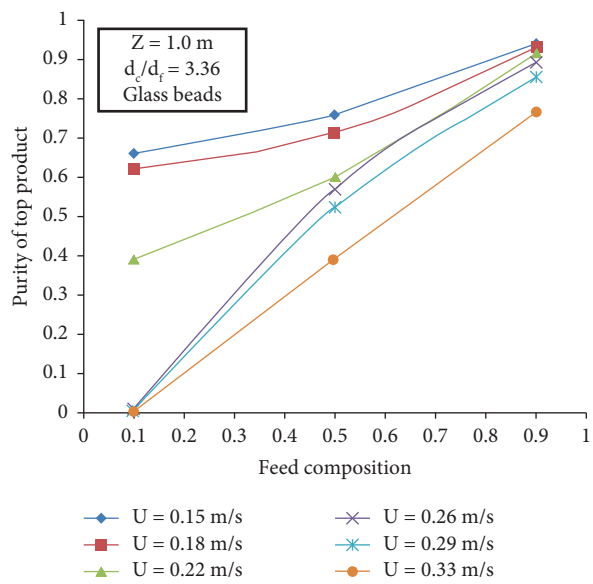

Figure 45: The influence of feed composition on the purity of top product at several liquid velocities.

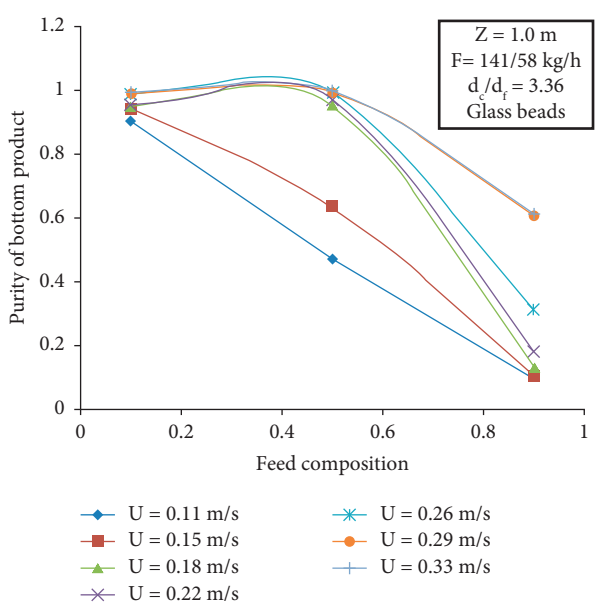

Figure 46: The influence of feed composition on the purity of the bottom product at several liquid velocities at the feed entrance.

The purity of the lower product increases with liquid velocity or solid feed rate and decreases with feed fine particle concentration as shown in the correlation equation as follows:

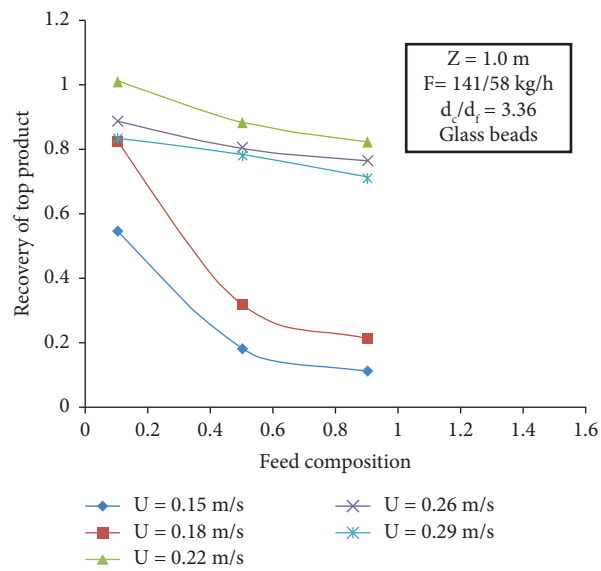

Figure 47: The influence of feed composition on the recovery of top product at several liquid velocities at the feed entrance.

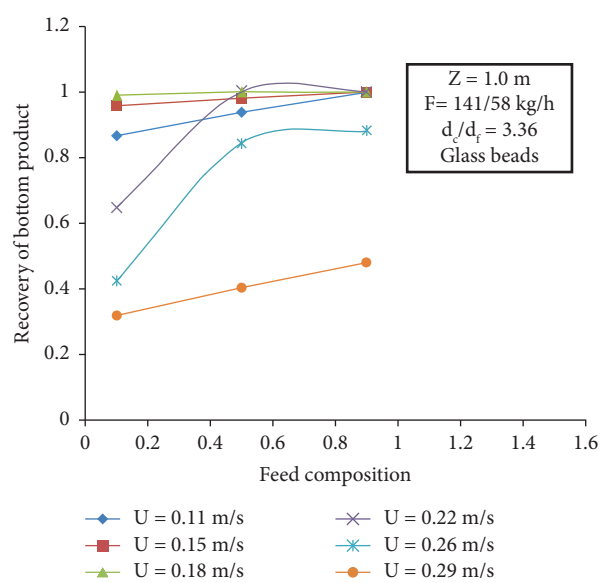

Figure 48: The influence of feed composition on the recovery of bottom products at several liquid velocities.

$$X_c = 0.273\left[\left(\frac{U_{t,c} - U_L}{U_{t,c} - U_{t,f}}\right)^{-0.03} (x_f)^{-0.54} \left(\frac{Z}{Z_0}\right)^{-0.014}\right. \quad (4)$$

All the correlations fit the experimental data with a deviation of less than 15%.

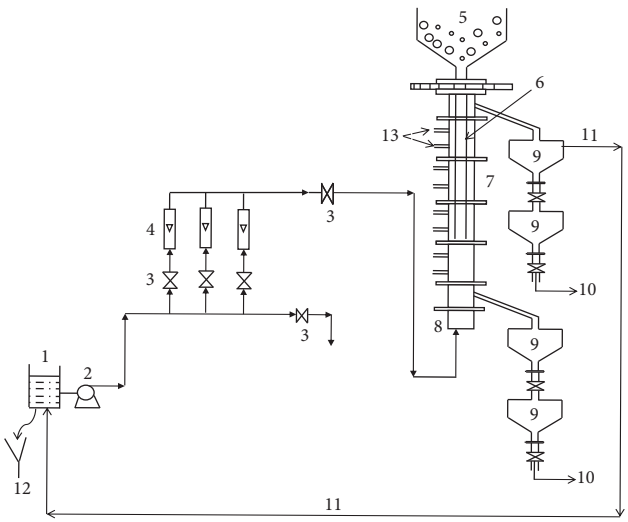

Figure 49: Experimental setup (1: water tank, 2: pump, 3: valves, 4: rotameter, 5: solid feeding tank, 6: feed pipe, 7: main column, 8: calming section, 9: solid collection tanks, 10: solid outlets, 11: recycle water, 12: drain, and 13: pressure taps).

4. Conclusions

The study centered on binary solid materials segregation including a significant amount of flotsam and jetsam. The binary combination characterized by a significant amount of miscellaneous and insignificant elements exhibited similar patterns, despite variations in size ratios. Segregation in continuous LFBs is influenced by several factors, including the rate at which solid material is introduced, the velocity of the liquid phase, the content of the feed, and the ratio of particle sizes. The removal rate of material and the quality of the resulting bottom product exhibit enhancement as the liquid velocity and solid input rate increase. However, this reduces material discharge and improves product quality. Feed composition changes increase top product purity and decrease bottom product purity. This study estimated top and bottom product entrainment, discharge rate, and purity using empirical correlations. The relationships were assessed using experimental data.

Nomenclature

d_p: Average diameter of the particles (m)
d_c: Diameter of coarser particles (m)
d_f: Diameter of fine particles (m)
F: Flow rate of feeding particles (kg/h)
E: Entrainment rate of solid materials (kg/h)
D: Discharge rate of solid materials (kg/h)
ρ_p: Density of the particles (kg/m^3)
ρ_L: Density of liquid (kg/m^3)
U_L: Liquid superficial velocity (m/s)
U_{mf}: Minimum fluidization velocity (m/s)
U_t: Terminal settling or transport velocity of particles (m/s)
$U_{t,f}$: Terminal settling or transport velocity of fine particles (m/s)
$U_{t,c}$: Terminal settling or transport velocity of coarser particles (m/s)
x_f: Fraction of finer components in the feed mixture
x_c: Fraction of coarser components in the feed mixture
Z: Feed pipe location length (m)
Z_o: Length of the active column (m)
X_c: The purity of coarser particles in the bottom product
X_f: The purity of fine particles in the top product
Y_c: The purity of coarser particles in top product
Y_f: The purity of fine particles in the top product.

Data Availability

The data used to support the findings of the study are included within the article.

Conflicts of Interest

The authors declare that they have no conflicts of interest.

Acknowledgments

The authors would like to thank the institute authorities for providing the facilities to carry out the project work.

References

[1] G. Van dujin and K. Riethma, "Segregation of liquid-fluidized solids," *Chemical Engineering Science*, vol. 37, no. 5, pp. 727–733, 1981.
[2] R. Di Felice, "Hydrodynamics of liquid fluidisation," *Chemical Engineering Science*, vol. 50, no. 8, pp. 1213–1245, 1995.
[3] A. Chen, J. R. Grace, N. Epstein, and C. J. Lim, "Steady state dispersion of mono-size, binary and multi-size particles in a liquid fluidized bed classifier," *Chemical Engineering Science*, vol. 57, no. 6, pp. 991–1002, 2002.
[4] K. P. Galvin, S. J. Pratten, and S. K. Nicol, "Dense medium separation using a teetered bed separator," *Minerals Engineering*, vol. 12, no. 9, pp. 1059–1081, 1999.
[5] S. Narasimha Reddy and P. S. T. Sai, "Continuous segregation of binary mixture of solids in liquid fluidised beds: influence of feed entry location," *Indian Chemical Engineer*, vol. 61, no. 2, pp. 153–166, 2019.
[6] S. Narasimha Reddy and P. S. T. Sai, "Continuous segregation of homogeneous binary mixture of solids by a liquid fluidised bed classifier," *Indian Chemical Engineer*, vol. 62, no. 1, pp. 28–39, 2020.
[7] G. Olivieri, A. Marzocchella, and P. Salatino, "Segregation of fluidized binary mixtures of granular solids," *AIChE Journal*, vol. 50, no. 12, pp. 3095–3106, 2004.
[8] S. Turrado, J. R. Fernández, and J. C. Abanades, "Investigation of the segregation of binary mixtures with iron-based particles in a bubbling fluidized bed," *ACS Omega*, vol. 4, no. 5, pp. 9065–9073, 2019.

[9] K. G. Palappan and P. S. T. Sai, "Studies on segregation of binary mixture of solids in a continuous fast fluidized bed," *Chemical Engineering Journal*, vol. 138, no. 3, pp. 358–366, 2008.

[10] K. Palappan and P. S. T. Sai, "Studies on segregation of binary mixture of solids in continuous fast fluidized bedPart III. Quantification of performance of the segregator," *Chemical Engineering Journal*, vol. 145, no. 1, pp. 100–111, 2008.

[11] S. M. Subhani and B. Srinivas, "Separation of mixtures in mass transfer applications by fluidization," *International Journal of Scientific Engineering and Research*, vol. 2, no. 4, pp. 107–114, 2014.